Journal of MATERIALS RESEARCH

Article
DOI: 10.1557/jmr.2020.320

Simple nanoindentation-based method for determining linear thermal expansion coefficients of micro-scale materials

Yuanbin Qin[1], Zhiyu Nie[1], Chao Ma[2], Longchao Huang[1], Yueqing Yang[1], Qinqin Fu[1], Weifeng He[3], Degang Xie[1,a)]

[1]Center for Advancing Materials Performance from the Nanoscale, State Key Laboratory for Mechanical Behavior of Materials, Xi'an Jiaotong University, Xi'an 710049, P.R. China
[2]Center for High Resolution Electron Microscopy, College of Materials Science and Engineering, Hunan University, Changsha 410082, P.R. China
[3]Science and Technology on Plasma Dynamics Laboratory, Air Force Engineering University, Xi'an 710038, P.R. China
[a)]Address all correspondence to this author. e-mail: dg_xie@xjtu.edu.cn

Received: 17 August 2020; accepted: 29 October 2020

The thermal expansion coefficient (CTE) is a vital design parameter for reducing the thermal-stress-induced structural failure of electronic chips/devices. At the micro- and nano-scale, the typical size range of the components in chips/devices, the CTEs are probably different from that of the bulk materials, but an easy and accurate measurement method is still lacking. In this paper, we present a simple but effective method for determining linear CTEs of micro-scale materials only using the prevalent nanoindentation system equipped with a heating stage for precise temperature control. By holding a constant force on the sample surface, while heating the sample at a constant rate, we measure two height–temperature curves at two positions, respectively, which are close to each other but at different heights. The linear CTE is obtained by analyzing the difference of height change during heating. This method can be applied to study the size effect or surface effect of CTE of embedded micro-scale structures, aiding the failure analysis and structural design in the semiconductor industry.

Introduction

With the development of micro-nano fabrication techniques, the size of semiconductor devices has been reduced rapidly and the application of micro- and nano-scale materials is more and more extensive, such as large-scale integrated circuits (IC), microelectromechanical systems (MEMS), light-emitting device, and electronics packaging [1]. One of critical factors that threatens the reliability of these chips/devices/systems is the mismatch of thermal expansion coefficient (CTE) between unit structures made of different materials, which introduces residual strain to not only affect the performance of devices but also cause deformation or even structural failure. On the other hand, many thermally driven MEMS devices depend significantly on the linear CTEs [2, 3]. Therefore, the accurate measurement of linear CTEs of micro- and nano-scale materials is vital for optimizing device structure, improving thermal stability and service life of devices. However, many studies show that the linear CTEs of micro- and nano-scale materials are not necessarily the same as that of the bulk materials. Taking TiN thin films with thickness of several micrometers as an example, the CTEs measured by Mayrhofer et al. are 6.8×10^{-6}–7.2×10^{-6} K^{-1} [4], and the result measured by Bielawski is 7.5×10^{-6} K^{-1} [5], which are quite different from the reported value of bulk materials, 9.35×10^{-6} K^{-1} [6]. Generally speaking, the mechanical properties of thin films depend upon the film thickness and the fabrication processes used [7, 8, 9, 10, 11, 12]. Hence, the CTEs of bulk materials cannot be directly used to simulate the thermal stress in devices with micro- and nano-scale structures. In this regard, an effective method for measuring the CTEs of micro- and nano-scale structures is urgent for the semiconductor industry.

Existing techniques are mainly used to measure CTEs of bulk material [13, 14, 15, 16, 17, 18, 19, 20], rather than micro- and nano-scale materials. Two most commonly used methods for measuring CTEs of micro- and nano-scale materials are X-ray diffraction (XRD) [21, 22] and thermally induced bending (TIB) [23]. The high measurement accuracy of the XRD method has been well recognized for crystalline

materials, but not for amorphous materials, or the micro- and nano-scale materials since obtaining high-quality diffraction patterns from these materials is very challenging. On the other hand, the expansion caused by defects cannot be measured by XRD. TIB is a method designed for measuring the CTEs of thin films. Unlike XRD, this method can provide comparable measurement accuracy for both crystalline and amorphous films, even for nano-scale films. However, the TIB method requires additional mechanical calculation to obtain the CTE values, making its accuracy dependent on input parameters such as Young's modulus/Poisson's ratio of both layer materials and the CTE of reference materials, whereas these parameters change themselves with size at small scales, which severely undermines the measurement reliability of the TIB method. In addition, the CTE measured by TIB refers to the in-plane component of the linear expansion thermal coefficient [24], so TIB is not suitable for anisotropic materials and materials without substrates. Recently, a method based on atomic force microscopy has been proved to be able to measure CTEs of polymers at the micro- and nano-scale [25, 26], but this method is sensitive to the surface condition of the sample and is very time-consuming. Moreover, it is impossible to continuously track the change of CTE with temperature. Other methods and techniques have also been proposed to determine the CTEs of micro- and nano-scale materials. However, none of the aforementioned methods for measuring the CTEs of micro-scale materials can simultaneously have merits of being easy to handle, accurate, reliable, and economical [27].

In this paper, we present a simple nanoindentation-based method for determining the linear CTEs of micro-scale materials. By using the nanomechanical test instrument equipped with high-temperature stage, we are able to measure the expansion of the sample upon heating. To eliminate the expansion of the testing system during heating, we measured the expansion twice at different positions of the sample with different height, and then the coefficient of thermal expansion can be calculated by using the difference between two measurements.

Measurement principle

Figure 1 schematically depicts the testing principle of our method. Firstly, the samples were prepared into wedge shape (a) or step shape (b) on the upper surface by mechanical thinning and polishing or electropolishing, and then were fixed onto the high-temperature stage of the nanomechanical test instrument. Two locations with a certain height difference are selected on the sample: test position 1 and test position 2. As shown in Fig. 1, the heights of the two locations are marked as h_1 and h_2, respectively. The height values can be directly read out by the nanomechanical test instrument, and the height difference is defined as $\Delta h = h_1 - h_2$. During heating, we can

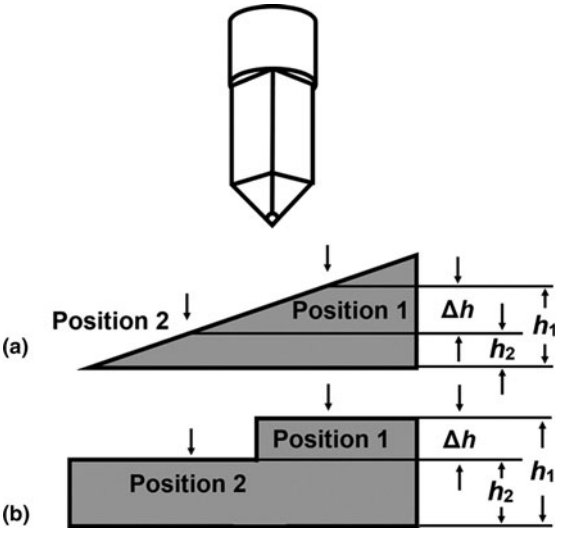

Figure 1: Schematic illustration of the experimental setup for measuring the CTEs based on nanoindentaion. The samples should be prepared into (a) wedge shape or (b) step shape.

measure the height changes of test positions 1 and 2 by using the transducer in the nanomechanical test instrument, which are recorded as Δh_1 and Δh_2, respectively. Then, the difference between Δh_1 and Δh_2 is the expansion of the sample with the thickness of Δh. The linear CTE α of the sample can be calculated through the following equation:

$$\alpha = \frac{\Delta h_1 - \Delta h_2}{\Delta h \Delta T} = k/\Delta h, \tag{1}$$

where ΔT is the change in temperature from the initial temperature T_0 to the elevated temperature T_f, and k is the slope of $\Delta h_1 - \Delta h_2$ versus temperature curve.

In this method, Δh_1 or Δh_2 is a combined result, determined by the expansion of the testing system, the creep of the sample, the thermal drift, and the expansion of the sample with the thickness of h_1 or h_2. As α was derived from $\Delta h_1 - \Delta h_2$, the expansion of the testing system including the heating stage and tip, and the creep of the sample can be eliminated. The only uncertainty worth noting comes from the thermal drift, which may be different in each test. This can be expressed by the following equations:

$$\Delta h_1 = d_{s1} - d_{c1} + d_{d1} + d_{e1}, \tag{2}$$

$$\Delta h_2 = d_{s2} - d_{c2} + d_{d2} + d_{e2}, \tag{3}$$

where d_s, d_c, d_d, and d_e are the displacements caused by the testing system, creep, thermal drift, and expansion of the sample, respectively. For the same testing system and the same sample, d_{s1} equals to d_{s2} and d_{c1} equals to d_{c2}, so

$$\Delta h_1 - \Delta h_2 = (d_{e1} - d_{e2}) + (d_{d1} - d_{d2}). \tag{4}$$

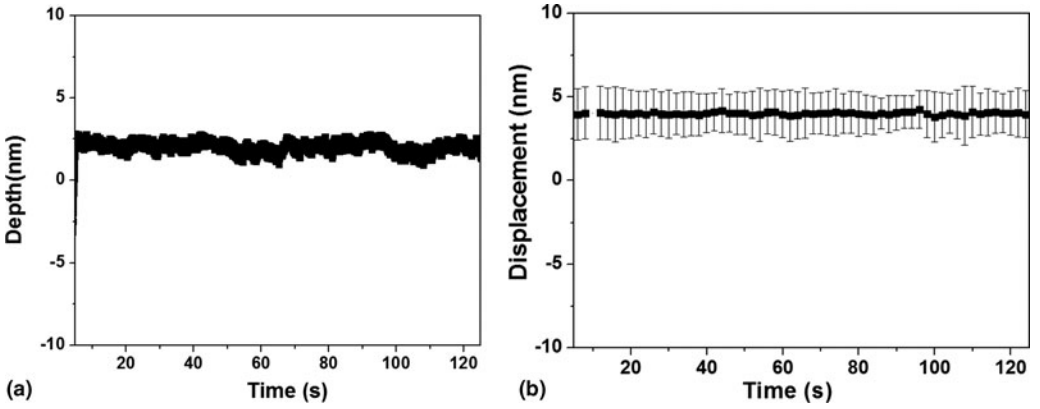

Figure 2: Measurement of thermal drift in our nanomechanical test instrument: (a) thermal drift corrected displacement as a function of time when the load of 2 μN is applied to the surface of the sample by the indenter and (b) average results of multiple measurements.

If the thermal drift is 0.05 nm/s, and the test time is 200 s, the displacement caused by thermal drift is 10 nm, which is very large for the expansion of materials at the micro-scale. For example, the CTE of aluminum is 23.2×10^{-6} °C^{-1} at room temperature, and if the thickness is 50 μm, the expansion will be only 23.2 nm when the temperature rises by 20 °C. Therefore, to guarantee the measurement accuracy, we must minimize the thermal drift or the fluctuation of the thermal drift during the test, as the instrument is able to remove the thermal drift. At the beginning of each test, a small load is applied to the surface of the sample by the indenter, and the displacement as a function of time is measured to calculate the thermal drift, which will be subtracted in the following test by the instrument automatically. As long as the drift remains constant during the test, the influence of drift on the test results can also be ignored, even if the drift is very large. Waiting for some time before the test is a good way to stabilize the drift. In our experiments, the thermal drift or its fluctuation can be easily reduced to a level as small as 0.01 nm/s, as shown in Fig. 2. Figure 2(a) shows the thermal drift corrected displacement as a function of time when a load of 2 μN is applied to the surface of the sample by the indenter at room temperature, exhibiting a thermal drift of about 0.002 nm/s. Furthermore, the error caused by thermal drift can be reduced by an average operation across multiple measurements. By doing this, the average thermal drift is only about 6×10^{-5} nm/s, as shown in Fig. 2(b). These results demonstrate a feasibility of our method in determining the CTEs of materials with the thickness down to micrometers or even below a micrometer.

Results and discussion

Scanning electron microscope (SEM) investigation and energy-dispersive X-ray (EDX) analysis were performed to check the chemical composition and surface morphology of these samples in our experiment. Figures 3(a)–3(c) show the EDX spectrums of the aluminum, titanium, and epoxy resin samples, respectively. The results show that both Al and Ti samples are pure metal without other elements detected. On the epoxy resin sample, C, O, Zr, and Cl elements are detected. The insets of Figs. 3(a)–3(c) are the SEM images showing the surface morphology of the samples after polishing.

The displacements as a function of temperature measured at position 1 and 2 (here, the height difference is about 56.0 μm) on the aluminum sample are shown in Figs. 4(a) and 4(b), respectively. At the beginning, there is a short period of displacement increase due to the creep, which is soon overwhelmed by the thermal expansion. When thermal expansion dominates, the displacement decreases nearly linearly with temperature change, indicating a constant increase in height. This phenomenon is more obvious in the tests with Ti, as shown in Figs. 4(d) and 4(e). To get an accurate result, three or four measurements have been performed at the same height of the sample. The difference between the displacements measured at two positions is the expansion of the aluminum with a thickness of 56.0 μm heated from 25 to 45 °C, shown in Fig. 4(c). Then, the CTE can be calculated using Eq. (1), which is about $(22.9 \pm 5.3) \times 10^{-6}$ °C^{-1}, which is consistent with the values of other measurement results and bulk materials [28, 29, 30] (see Table 1). Because of the effect of thermal drift or possible different creep rates at different positions, the relationship between $\Delta h_1 - \Delta h_2$ and temperature is not strictly linear, as shown in Fig. 4(c). This disadvantage is more obvious at smaller Δh and ΔT. The larger Δh and ΔT, the more accurate the CTE we measured is, and we believe that we can get a more accurate CTE if we carry out more experiments. Similar experiments were performed on a titanium sample, and the results are shown in Figs. 4(d)–4(f). The CTE of the titanium sample with a thickness of 90.3 μm from 30 to 50 °C is $(11.6 \pm 1.5) \times 10^{-6}$ °C^{-1}, which is consistent with the values of other measurement results and bulk materials [29, 31] (see

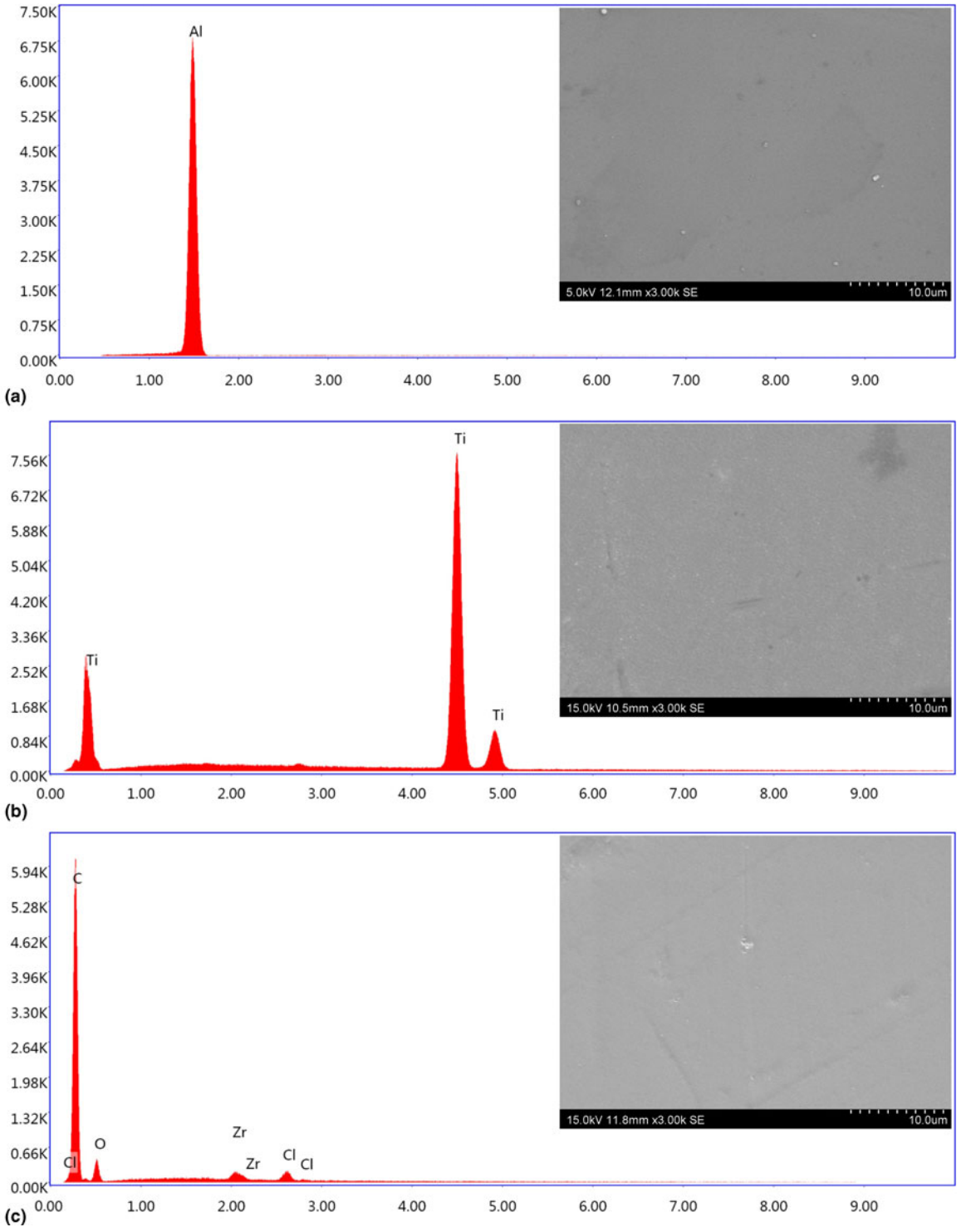

Figure 3: EDX spectrums of the (a) aluminum, (b) titanium, and (c) epoxy resin samples, respectively. The insets of (a)–(c) are the corresponding SEM images showing the surface morphology of the samples after polishing.

Table 1), and the difference is probably from the effect of thermal drift or possible different creep rates at different positions.

Similar experiments were also performed on an epoxy resin sample, and the results are shown in Fig. 5. First, the measurements were performed in different temperature ranges from 30 to 40 °C, from 40 to 50 °C, and from 50 to 55 °C, shown in Figs. 5(a)–5(c), respectively. Then, these displacement–temperature relations at different temperature ranges were pieced up to form a single one covering a larger temperature range, as shown in Fig. 5(d). Within the temperature range, we found

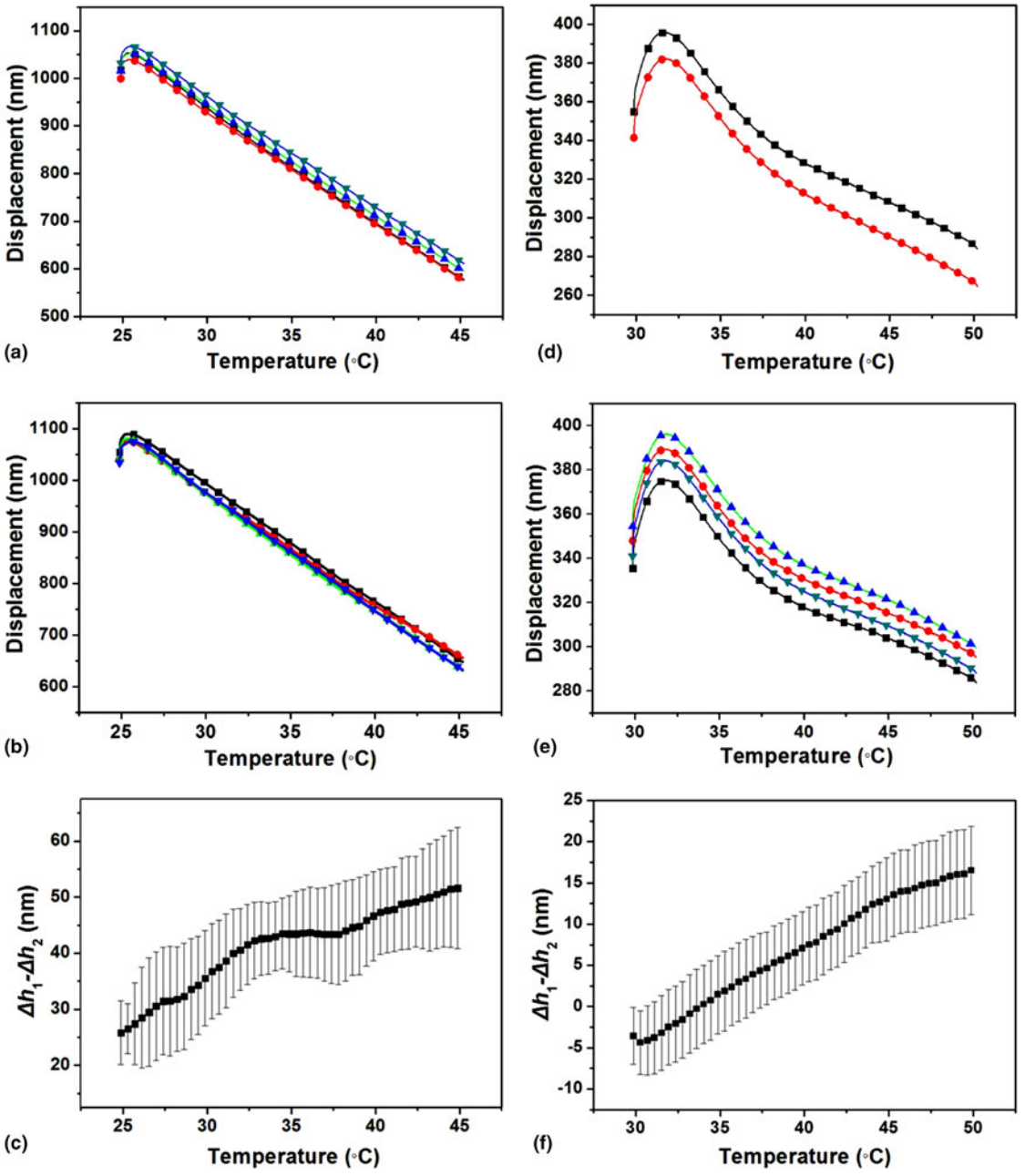

Figure 4: Displacement as a function of temperature measured at (a) position 1 and (b) position 2 on the Al sample heated from 25 to 45 °C. Each curve represents one measurement. (c) Average difference between the displacements measured at position 1 and position 2 on the Al sample heated from 25 to 45 °C. Displacement as a function of temperature measured at (d) position 1 and (e) position 2 on the Ti sample heated from 30 to 50 °C. Each curve represents one measurement. (f) Average difference between the displacements measured at position 1 and position 2 on the Ti sample heated from 30 to 50 °C.

a glass transition occurred at about 50 °C. The CTEs before and after glass transition are $(217 \pm 31) \times 10^{-6}$ °C^{-1}, averaged over the temperature range 31–50 °C, and $(749 \pm 31) \times 10^{-6}$ °C^{-1}, averaged over the temperature range 51–54 °C, respectively. The CTE before glass transition is much larger than the value of bulk epoxy resin, which is about 80×10^{-6} °C^{-1}, showing strong size effect, which is consistent with Feng et al. [26, 32]. The CTE of epoxy resin at micro-scale before glass transition is larger by a factor of approximately 2.7 than the value for bulk epoxy resin. In Feng's study [31], to get the out-of-plane CTE (α_2) of an epoxy coating, the in-plane CTE (α_1) and volumetric CTE (α_v) had to be measured first and then α_2 could be calculated through the following equation:

$$\alpha_2 = \alpha_v - 2\alpha_1. \quad (5)$$

Obviously, this is more complicated compared with our method, and due to the error accumulation effect, the

TABLE 1: CTEs of Al and Ti in our study, compared with other measurement results and bulk materials.

Samples	Linear CTEs ($\times 10^{-6}$ °C^{-1})
Al (56.0 μm) this work	22.9 ± 5.3
Al (15 μm) [29]	24.6
Bulk Al [30]	24.0
Tl (90.3 μm) this work	11.6 ± 1.5
Ti (3.2 μm) [29]	8.79 (transverse direction), 9.16 (rolling direction)
Bulk Ti [31]	9.5

out-of-plane CTE has a higher degree of uncertainty when compared with the in-plane property.

The size effect of CTE of epoxy resin can be explained by the intramolecular and intermolecular forces of the polymer molecules [33]. Choy mentioned that when the majority forces in the molecules are weak Van der Waals forces, the material will show a larger CTE in the order of 10^{-4} °C^{-1} (in the range of several hundred ppm °C^{-1}) [34]. However, if the molecules are held by strong covalent bonds, the materials will show a much smaller CTE in the order of 10^{-6} °C^{-1} (in the range of several ppm °C^{-1}). Actually, all epoxy resin samples contain both weak Van der Waals bonds and strong covalent bonds in certain proportion, and size scale is one important factor to affect the proportion of different bonds. Compared with bulk epoxy resin, micro-scale epoxy resin has a higher proportion of Van der Waals forces, due to its abundant surface area which makes the intermolecular covalent bonding vulnerable under external physical stimulus. For example, covalent bonds can be easily destroyed by mechanical polishing. Consequently, the higher CTE measured in the micro-scale epoxy resin can be explained by fewer proportion of strong covalent bonds.

Conclusion

In summary, based on the nanoindentation technique, a simple and novel method for determining linear CTEs of micro-scale materials has been developed. The principle of our method is based on the original definition of thermal expansion, making it simple and easy to understand, just like traditional method for bulk materials. This method is applicable to most solid-state materials, including crystalline and amorphous materials with or without substrates, and requires only easy sample preparation step to fabricate wedge or step-shaped area on the surface. Compared with the widely used TIB, our method does not need the input of other mechanical/thermal parameters for

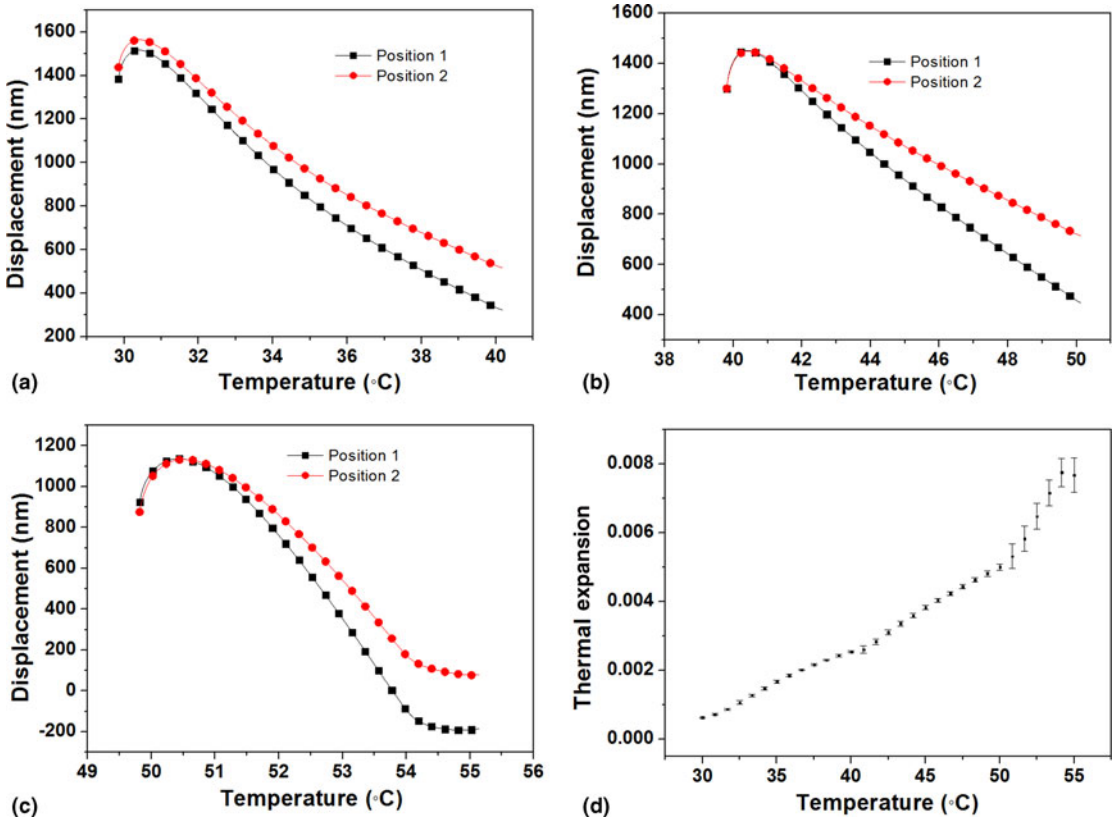

Figure 5: (a) Typical displacement as a function of temperature measured at position 1 and position 2 on the epoxy resin sample heated from 30 to 40 °C. (b) Typical displacement as a function of temperature measured at position 1 and position 2 on the epoxy resin sample heated from 40 to 50 °C. (c) Typical displacement as a function of temperature measured at position 1 and position 2 on the epoxy resin sample heated from 50 to 55 °C. (d) Thermal expansion as a function of temperature for epoxy resin at micro-scale.

calculating the CTE, also with the advantage of measuring the out-of-plane CTE. The method was demonstrated for the measurement of CTEs in micro-scale Al and Ti samples, and the results are in good agreement with the reported data measured by other methods. For polymer materials, our results with epoxy resin show a much higher CTE in the micro-scale sample than in the bulk sample, demonstrating a strong size effect of CTE in polymers. Considering the pervasive presence of micro- and nano-scale structures of various types of materials in IC chips and other miniature devices, there shall be huge needs for such kind of CTE measurement of small-scale materials to improve the reliability of thermomechanical analysis or aid the structural optimization in design.

Experiments

The CTEs of single-crystalline aluminum (Al, Goodfellow Cambridge Limited, Cambridge, United Kingdom; 99.99%) and polycrystalline titanium (Ti, ELETMENT TECH MATERIAL Co., Ltd, Weihai, P. R. China; 99.999%) have been measured by our method, which are well consistent with the values from other methods. Aluminum and titanium were chosen, as they are widely used and their CTEs show mild size-dependent effect. The Al sample was prepared into wedge shape by mechanical polishing and followed by electropolishing. The length was about 3.0 mm, and the width is about 2.0 mm. The maximum and minimum heights of the sample are about 0.5 and 0.2 mm, respectively. The Ti sample was prepared into wedge shape by mechanical thinning and polishing from a bulk cylindrical sample. The cross section of the Ti sample is a circle with diameter about 8.0 mm. The maximum and minimum heights of the sample are about 2.0 and 1.0 mm, respectively. The samples were fixed onto the high-temperature stage of the nanomechanical test instrument by silver paint. After that, our method was applied to study the thermal expansion of epoxy resin, an amorphous polymer. Epoxy resin plays a vital role in electronic packages because of its ease of processing, low cost, low dielectric constant, low shrinkage, excellent corrosion resistance, adhesive properties, and electrical insulation performance [35]. Since many filled epoxy resins between integrated circuit or die and the substrate in ICs are about 100 μm thick [36], it is necessary to measure the CTE of epoxy resin at micro-scale. The epoxy resin was prepared using EpoFix Kit produced by Struers Ltd. The EpoFix resin and EpoFix hardener were mixed according to the weight ratio of 25:3, and then put into a vacuum tank for more than 12 h, so as to reduce the bubbles in the epoxy resin. After the epoxy resin sample was prepared into wedge shape or cuboid by the mechanical method, the sample was heated to above 100 °C and cooled slowly to reduce the effect of stress in the process of sample preparation, so as to obtain a uniform sample. The CTE of bulk epoxy resin (20.9 mm × 6.4 mm × 4.3 mm) was measured using a NETZSCH DIL 402C thermal dilatometer, and the heating rate is 5 °C/min. The length of the epoxy resin sample for the measurement at micro-scale was about 10.0 mm, and the width is about 5.0 mm. The maximum and minimum heights of the sample are about 2.0 and 0.5 mm, respectively. The chemical composition was checked using EDX semiquantitative analysis on a Hitachi SU6600 SEM. The measurements of CTEs of materials in the micro-scale were performed on a Hysitron TI-950 TriboIndenter equipped with high-temperature stage xSol 800. A nanoDMA transducer with a Berkovich probe and a dynamic creep testing technique was employed, whereby a small oscillation at a particular reference frequency (220 Hz in this case) was superimposed onto the quasi-static load function, which is only for the convenience of data processing. A peak load of 8 mN was used and held for 240 s, with simultaneous heating from 25 to 45 °C for Al (30–50 °C for Ti), for both the tip and the sample, at heating rate 5 °C/min. Due to the limited displacement range of the transducer and the significant change of mechanical property of epoxy resin during heating, three measurements in different temperature ranges were performed. A peak load of 10 mN was used and held for 120 s, with simultaneous heating from 30 to 40 °C with heating rate of 5 °C/min. Other combinations of peak loads, holding time, and heating temperatures were also applied, such as 8 mN for 120 s from 40 to 50 °C and 4 mN for 60 s from 50 to 55 °C.

Acknowledgment

The author gratefully thanks Professor Zhiwei Shan, Professor Boyu Liu, and Professor Kai Chen at Xi'an Jiaotong University for the valuable discussions.

References

1. **H.P. Chi**: A simple method for determining linear thermal expansion coefficients of thin films. *J. Micromech. Microeng.* **12**, 548 (2002).
2. **P. Lerch, C.K. Slimane, B. Romanowicz, and P. Renaud**: Modelization and characterization of asymmetrical thermal micro-actuators. *J. Micromech. Microeng.* **6**, 134 (1996).
3. **C.S. Pan and W. Hsu**: An electro-thermally and laterally driven polysilicon microactuator. *J. Micromech. Microeng.* **7**, 7 (1997).
4. **P.H. Mayrhofer, F. Kunc, J. Musil, and C. Mitterer**: A comparative study on reactive and non-reactive unbalanced magnetron sputter deposition of TiN coatings. *Thin Solid Films* **415**, 151 (2002).
5. **M. Bielawski**: Residual stress control in TiN/Si coatings deposited by unbalanced magnetron sputtering. *Surf. Coat. Technol.* **200**, 3987 (2006).

6. **H.O. Pierson**: *Handbook of Refractory Carbides and Nitrides: Properties, Characteristics, Processing and Applications* (Noyes Publications, NJ, USA, 1996), p. 186.
7. **W. Fang and J.A. Wickert**: Comments on measuring thin-film stresses using bi-layer micromachined beams. *J. Micromech. Microeng.* **5**, 276 (1995).
8. **W. Fang and C.-Y. Lo**: On the thermal expansion coefficients of thin films. *Sens. Actuators A* **84**, 310 (1999).
9. **M. Von Arx, O. Paul, and H. Baltes**: Process-dependent thin-film thermal conductivities for thermal CMOS MEMS. *J. Microelectromechan. Syst.* **9**, 136 (2000).
10. **W. Fang and J.A. Wickert**: Determining mean and gradient residual stresses in thin films using micromachined cantilevers. *J. Micromech. Microeng.* **6**, 301 (1996).
11. **J.J. Vlassak and W.D. Nix**: A new bulge test technique for the determination of Young's modulus and Poisson's ratio of thin films. *J. Mater. Res.* **7**, 3242 (1992).
12. **E. Jansen and E. Obermeier**: Thermal conductivity measurements on thin films based on micromechanical devices. *Diam. Relat. Mater.* **5**, 644 (1996).
13. **R.V. Jones and J.C.S. Richards**: Recording optical lever. *J. Sci. Instrum.* **36**, 90 (1959).
14. **R.E. Kinzly**: A new interferometer capable of measuring small optical path differences. *Appl. Opt.* **6**, 137 (1967).
15. **S.F. Jacobs, J.N. Bradford, and J.W. Berthold**: Ultraprecise measurement of thermal coefficients of expansion. *Appl. Opt.* **9**, 2477 (1970).
16. **Y. Okada and Y. Tokumaru**: Precise determination of lattice parameter and thermal expansion coefficient of silicon between 300 and 1500 K. *J. Appl. Phys.* **56**, 314 (1984).
17. **G. Fug, H. Gasparoux, and J.J. Piaud**: Thermal variation apparatus for X-ray diffraction experiments up to 3000 K. *J. Phys. E Sci. Instrum.* **5**, 1222 (1972).
18. **S. Miksic, G. Sherman, and H. Lal**: High-temperature X-ray diffraction furnace using a thermal-image technique. *J. Appl. Crystallogr.* **9**, 466 (1976).
19. **K.G. Lyon, G.L. Salinger, C.A. Swenson, and G.K. White**: Linear thermal expansion measurements on silicon from 6 to 340 K. *J. Appl. Phys.* **48**, 865 (1977).
20. **Y. Okada**: A high-temperature attachment for precise measurement of lattice parameters by Bond's method between room temperature and 1500 K. *J. Phys. E Sci. Instrum.* **15**, 1060 (1982).
21. **K.S. Gadre and T.L. Alford**: Crack formation in TiN films deposited on Pa-n due to large thermal mismatch. *Thin Solid Films* **394**, 124 (2001).
22. **Y. Zoo, D. Adams, J.W. Mayer, and T.L. Alford**: Investigation of coefficient of thermal expansion of silver thin film on different substrates using X-ray diffraction. *Thin Solid Films* **513**, 170 (2006).
23. **A. Champi, R.G. Lacerda, G.A. Viana, and F.C. Marques**: Thermal expansion dependence on the sp^2 concentration of amorphous carbon and carbon nitride. *J. Non Cryst. Solids* **338–340**, 499 (2004).
24. **E. Besozzi, D. Dellasega, A. Pezzoli, A. Mantegazza, M. Passoni, and M.G. Beghi**: Coefficient of thermal expansion of nanostructured tungsten based coatings assessed by substrate curvature method. *Mater. Des.* **137**, 192 (2018).
25. **D. Olmos, F. Martínez, G. González-Gaitano, and J. González-Benitoa**: Effect of the presence of silica nanoparticles in the coefficient of thermal expansion of LDPE. *Eur. Polym. J.* **47**, 1495 (2011).
26. **X.R. Zhang, T.S. Fisher, A. Raman, and T.D. Sands**: Linear coefficient of thermal expansion of porous anodic alumina thin films from atomic force microscopy. *Nanosc. Microsc. Thermophys. Eng.* **13**, 243 (2009).
27. **J. González-Benito, E. Castillo, and J.F. Cruz-Caldito**: Determination of the linear coefficient of thermal expansion in polymer films at the nanoscale: Influence of the composition of EVA copolymers and the molecular weight of PMMA. *Phys. Chem. Chem. Phys.* **17**, 18495 (2015).
28. **J.H. Zhao, Y. Du, M. Morgen, and P.S. Ho**: Simultaneous measurement of Young's modulus, Poisson ratio, and coefficient of thermal expansion of thin films on substrates. *J. Appl. Phys.* **87**, 1575 (2000).
29. **A.M. Russell and B.A. Cook**: Coefficient of thermal expansion anisotropy and texture effects in ultra-thin titanium sheet. *Scr. Mater.* **37**, 1461 (1997).
30. **M.M.D. Lima, R.G. Lacerda, J. Vilcarromero, and F.C. Marques**: Coefficient of thermal expansion and elastic modulus of thin films. *J. Appl. Phys.* **86**, 4936 (1999).
31. **W. Riethmuller and W. Benecke**: Thermally excited silicon microactuators. *IEEE Trans. Electron Devices* **35**, 758 (1988).
32. **R. Feng and R.J. Farris**: The characterization of thermal and elastic constants for an epoxy photoresist SU8 coating. *J. Mater. Sci.* **37**, 4793 (2002).
33. **H.C. Liou, P.S. Ho, and R. Stierman**: Thickness dependence of the anisotropy in thermal expansion of PMDA-ODA and BPDA-PDA thin films. *Thin Solid Films* **339**, 68 (1999).
34. **C.L. Choy**: Chapter 4 Thermal expansivity of oriented polymers. In *Developments in Oriented Polymers-1*, I.M. Ward, ed. (Applied Science Publishers, London and NJ, England and USA, 1982), pp. 121.
35. **S. Liu, V.S. Chevali, Z. Xu, D. Hui, and H. Wang**: A review of extending performance of epoxy resins using carbon nanomaterials. *Compos. Part B* **136**, 197 (2018).
36. **S. Rimdusit and H. Ishida**: Development of new class of electronic packaging materials based on ternary systems of benzoxazine, epoxy, and phenolic resins. *Polymer* **41**, 7941 (2000).